Available online at www.sciencedirect.com
SCIENCE DIRECT®
Catalysis Today 91–92 (2004) 305–309
CATALYSIS TODAY
www.elsevier.com/locate/cattod

Preparation method and structure of active sites of FeO_x/SiO_2 catalysts in methane to formaldehyde selective oxidation

F. Arena [a], G. Gatti [b], S. Coluccia [b], G. Martra [b], A. Parmaliana [a,*]

[a] *Dipartimento di Chimica Industriale e Ingegneria dei Materiali, UNIME, Salita Sperone 31, I-98166 St. Agata, Messina, Italy*
[b] *Dipartimento di Chimica IFM, UNITO, Via P. Giuria 7, I-10125 Torino, Italy*

Abstract

The effects of preparation method on surface structures and catalytic properties in the selective oxidation of CH_4 to HCHO with O_2 (MPO) of low-loaded (0.09–0.43 wt.% Fe) FeO_x/SiO_2 catalysts have been addressed. The DR-UV-Vis patterns prove that the preparation route, based on "adsorption–precipitation" of Fe^{II} precursors on silica under anaerobic conditions (ADS/PRC), enhances the dispersion of the active phase in comparison to the conventional "incipient-wetness" route. FTIR of adsorbed NO data signal the presence on silica of several "isolated" Fe moieties with a different surface coordination. A higher FeO_x dispersion confers a superior performance to ADS/PRC FeO_x/SiO_2 catalysts in terms of specific rate of CH_4 conversion (σ_{CH_4}) and HCHO formation (ε_{HCHO}) of Fe atoms which result in quite larger HCHO productivity values (STY_{HCHO}).

Keywords: FeO_x/SiO_2 catalyst; Selective oxidation; Fe^{II} precursor

1. Introduction

A considerable amount of research work has been devoted during the last two decades to the investigation of supported iron-based systems as effective catalytic materials for the activation of molecular oxygen [1–8]. Most of catalyst formulations include zeolites as carrier, entailing a high dispersion of Fe^{III} ions into the matrix framework [1–3]. Moreover, FeO_x/SiO_2 catalysts feature an enhanced reactivity in the partial oxidation of CH_4 to CH_3OH/HCHO with O_2 (MPO) [4–9]. In turn, the functionality of FeO_x/SiO_2 catalysts in MPO depends upon concentration and structure of active sites, as "isolated" Fe species in a *tetrahedral-like* coordination mostly drive selective oxidation, while Fe_2O_3 *nanoparticles* lead to CO_x, owing to a high availability and mobility of lattice oxygen under reaction conditions [4–9].

Besides progress on catalyst optimisation, systematic studies on the steady-state gas–solid interactions aimed at elucidating the mechanism and kinetics of the MPO on silica-based catalysts, have been reported recently [9]. Namely, developing a formal kinetic model which describes the steady-state condition and activity–selectivity pattern of MPO catalysts, we provided scientific basis to catalyst optimisation and process design [9]. Then, on the basis of both theoretical predictions [9] and experimental findings [5–8], pointing to *dispersion* as a key-factor controlling the catalytic performance [5–14], a preparation route of FeO_x/SiO_2 catalysts ensuring a superior functionality in MPO was adopted [5–7].

Therefore, this paper is aimed at providing basic insights into the efficiency of the "adsorption–precipitation" (ADS/PRC) preparation method in promoting dispersion and catalytic behaviour of the FeO_x/SiO_2 system in MPO.

2. Experimental

2.1. Catalysts preparation

A series of FeO_x/SiO_2 catalysts (*FS-x*) was prepared by "adsorption–precipitation" of Fe^{II} ions under anaerobic conditions at pH of 7–8 (ADS/PRC) [5–7], using powdered Si 4-5P and F5 (*Akzo Nobel*) silicas as carrier and $FeSO_4$ precursor. For comparison, a series of catalysts (*x-FS*) was

* Corresponding author. Tel.: +39-090-676-5606; fax: +39-090-391518.
E-mail address: adolfo.parmaliana@unime.it (A. Parmaliana).

0920-5861/$ – see front matter © 2004 Elsevier B.V. All rights reserved.
doi:10.1016/j.cattod.2004.03.049

Table 1
List of SiO_2 samples and FeO_x/SiO_2 catalysts

Code	SiO_2 support	Preparation method—Fe precursor	Fe loading (wt.%)	SA_{BET} ($m^2\,g^{-1}$)	SL[a] ($Fe_{at}\,nm^{-2}$)
Si 4-5P	Si 4-5P	–	0.02	385	0.011
F5	F5	–	0.015	607	0.003
1-FS	F5	INC/WET—Fe^{III}	0.095	402	0.027
2-FS	Si 4-5P	INC/WET—Fe^{III}	0.10	402	0.027
3-FS	Si 4-5P	INC/WET—Fe^{III}	0.43	398	0.118
FS-1	Si 4-5P	ADS/PRC—Fe^{II}	0.350	399	0.096
FS-2	F5	ADS/PRC—Fe^{II}	0.095	601	0.016
FS-3	F5	ADS/PRC—Fe^{II}	0.370	597	0.068

[a] Surface Fe loading.

prepared by a conventional "incipient-wetness" (INC/WET) route using $Fe(NO_3)_3$ precursor [8]. After impregnation, all the catalysts were dried at 100 °C and then calcined at 600 °C (6 h). The list of catalysts is reported in Table 1.

2.2. IR measurements

Were carried out with a Bruker Equinox 55 instrument equipped with a DTGS detector and running at 4 cm^{-1} resolution. Samples were placed in a cell with KBr windows, allowing all thermal treatments and adsorption–desorption experiments to be carried out in situ. Spectra are reported in absorbance after subtraction of the IR pattern of the sample before NO adsorption ("blank" spectrum).

2.3. UV-Vis diffuse reflectance (DR-UV-Vis)

Spectra of the samples in powder form, contained in a cell with an optical quartz window, were acquired using a Perkin-Elmer Lambda 900 instrument equipped with an integrating sphere. The spectra, recorded in reflectance mode, were transformed using the "Kubelka-Munk" function.

2.4. Catalyst testing

In the MPO reaction was performed by a recirculation batch reactor operating at 650 °C and 1.7 bar with a flow rate of 1000 STP mL min^{-1} ($He:N_2:CH_4:O_2 = 6:1:2:1$) and a catalyst sample of 0.05 g, unless otherwise specified [4–8].

3. Results and discussion

3.1. Surface structures of FeO_x/SiO_2 catalysts

A basic investigation of the iron oxide dispersion on the various ADS/PRC and INC/WET FeO_x/SiO_2 catalysts was performed by recording the DR-UV-Vis spectra of the calcined samples in air. Under such conditions, all surface Fe ions have an octahedral coordination and, further to the calcination treatment at 600 °C, their ON is +3 [10]. The spectra of the various FeO_x/SiO_2 samples, normalised to the maximum intensity to better evidence the differences in bands' position, are shown in Fig. 1. The 1-FS sample (spectrum a), containing ca. 0.1 wt.% of Fe loaded by the INC/WET route on the Si 4-5P carrier, exhibits a weak ligand to metal charge transfer (CT) band in the 18 000–25 000 cm^{-1} range, indicating the presence of *Fe_2O_3 nanoparticles*, and a main CT absorption, with the onset at ca. 30 000 cm^{-1}, related to clustered grafted Fe species [10], likely forming extended *bi-dimensional patches* on the silica surface. In the case of the FS-1 sample (spectrum b), bearing a higher concentration of Fe (0.35 wt.%) by the ADS/PRC method on the above silica, a band in similar position monitors the presence of the latter species, while only traces of the component due to Fe_2O_3 *nanoparticles* are observable. Evidently such data are diagnostic of a great efficiency of the ADS/PRC route in favouring a selective adsorption of Fe^{II} ions on negatively polarised hydroxyl groups of the silica surface, preventing thus an extensive formation of 3D Fe_2O_3 aggregates during calcination [5–7]. The former signal is absent in the spectra of FS-2 and FS-3 samples (c and d, respectively), which exhibit a main band at higher wavenumber as the Fe loading decreases, namely falling in a range typical of the CT transition of *mono-*, *di-*, and *oligo-meric* Fe–O ligand species [10]. Then, the efficiency of the preparation routes is somewhat affected by the physico-chemical features of carriers.

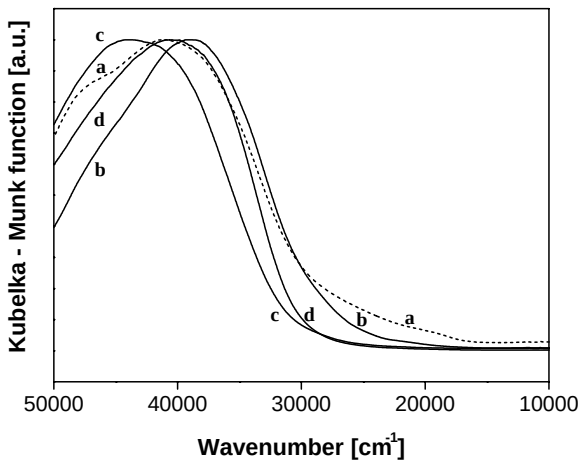

Fig. 1. DR-UV-Vis spectra of calcined FeO_x/SiO_2 catalysts in air, normalised to the maximum intensity: (a) 1-FS; (b) FS-1; (c) FS-2; (d) FS-3.

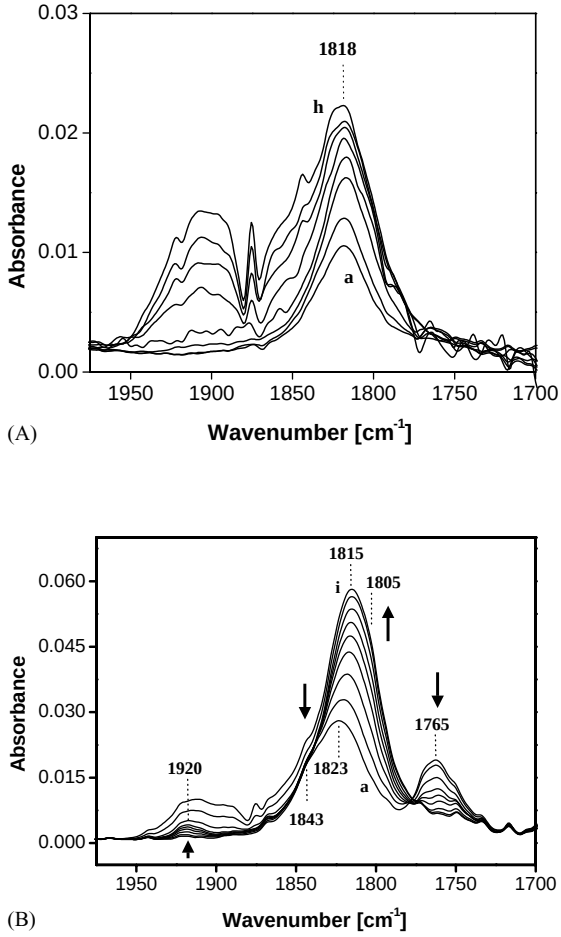

Fig. 2. (A) IR spectra of adsorbed NO at increasing NO pressures (6.5 Pa (a) to 2000 Pa (h)) on the FS-2 sample outgassed at 400 °C for 1 h. (B) IR spectra of adsorbed NO at increasing NO pressures (6.5 Pa (a) to 2000 Pa (i)) on the FS-3 sample outgassed at 400 °C for 1 h.

In order to obtain further insights into the structure of active sites at the highest level of dispersion, FTIR measurements of adsorbed NO were carrier out on the latter samples. It must be noticed that the preventive outgassing treatment at 400 °C in situ implies an almost overall conversion of surface Fe^{III} into Fe^{II} ions [5], as also confirmed by DR-UV-Vis and IR measurements of adsorbed CO (results not reported for the sake of brevity). Then, the spectra of adsorbed NO (6.5–2000 Pa) on the FS-2 (A) and FS-3 (B) samples are shown in Fig. 2. The admission of the first dose of NO on the FS-2 sample (Fig. 2A) produces a single band at 1818 cm^{-1}, due to mononitrosylic Fe(II)–NO adducts [11], while an increase of the NO coverage results in a rising intensity of this band and appearance of the roto-vibrational pattern of NO in the gas phase. These data indicate that Fe^{II} sites with only one coordinative vacancy are present on such system. By contrast, besides to a main component at 1823 cm^{-1}, due to mononitrosylic adducts, a shoulder at 1843 cm^{-1} and a band at 1765 cm^{-1} in the spectrum of the FS-3 sample at the lowest NO coverage (Fig. 2B, a) correspond to the symmetric-antisymmetric stretching modes of dinitrosylic Fe(II)–$(NO)_2$ adducts, respectively [11]. By increasing the amount of adsorbed NO, in fact, these two components progressively decrease in intensity transforming into two other signals, one, quite weak, at 1920 cm^{-1}, and the other, at ca. 1805 cm^{-1}, appearing as a shoulder of the main peak at 1815 cm^{-1}. These spectral features monitor the symmetric and antisymmetric stretching modes, respectively, of trinitrosylic Fe(II)–$(NO)_3$ adducts [13], formed by the additional insertion of a NO molecule on dinitrosyl adducts. Further, the increase of the NO coverage yields an increased intensity of the mononitrosylic band, the maximum of which shifts to lower frequency because of the disappearance of the shoulder at 1843 cm^{-1} and growth of that at 1805 cm^{-1}. The simultaneous presence of mono- and polynitrosylic adducts indicates that, in addition to Fe^{II} centres with only one coordinative vacancy, Fe^{II} sites with a higher degree (two- and/or three-fold) of coordinative unsaturation are present at the surface of the FS-3 catalyst.

3.2. Active sites and catalytic pattern in MPO of FeO_x/SiO_2 catalysts

The prediction of the requirements of MPO catalysts is a rather complicated task because of the low reactivity of CH_4 molecule and the high temperature essential for its activation, involving an easy occurrence of secondary reactions [4,9,12–15]. In this respect, literature findings suggest that a *proper* design of MPO catalysts must entail a high dispersion of transition metal ions, able to generate *active oxygen species*, over an "inert" matrix characterised by a medium/weak Brönsted-type acidity [4,9,12–17]. Namely, this points to the concept of "*site isolation*" [9,12–18], early invoked to state that a selective oxidation requires a proper ensemble of sites driving the activation of the substrate [9,12–18] while a high mobility and availability of nucleophylic lattice O^{2-} species, typical of oxide crystal lattices [9,12–14], is detrimental for the lifetime of intermediates. Controlling the speciation of active sites, then, it is expected that the preparation method confers a quite different catalytic functionality in MPO to FeO_x/SiO_2 systems [4–9]. In other words, a comparison of the performance of INC/WET and ADS/PRC catalysts allows to get further insights into the effect of the preparation route on dispersion of the active phase. Catalytic activity data of *x*-FS and FS-*x* samples at 650 °C, with reference to Si 4-5P and F5 silicas, are presented in Table 2 in terms of hourly CH_4 conversion (X_h, %), selectivity (S_X, %), productivity (STY_{HCHO}, $g\,kg_{cat}^{-1}\,h^{-1}$), and specific rate of CH_4 conversion (σ_{CH_4}, s^{-1}) and HCHO formation (ε_{HCHO}, s^{-1}) of Fe atoms, on the basis of the analytical loading (Table 1). The bare Si 4-5P silica features an hourly CH_4 conversion of 3.5% coupled to an S_{HCHO} of 78% accounting for an STY_{HCHO} of 310 $g\,kg_{cat}^{-1}\,h^{-1}$. As its lower Fe content (Table 1), the F5 silica features a lower activity (X_h, 2.9%) and an S_{HCHO} of 64%, resulting in an STY_{HCHO} of 200 $g\,kg_{cat}^{-1}\,h^{-1}$. Both silicas, likely characterised by the highest FeO_x dispersion [7], exhibit analogous σ_{CH_4} values

Table 2
Activity data of FeO_x/SiO_2 catalysts in MPO (T, 650 °C)[a]

Sample	w_{cat} (mg)	X_h (%)[b]	S_{HCHO} (%)	S_{CO} (%)	S_{CO_2} (%)	σ_{CH_4} (s^{-1})	ε_{HCHO} (s^{-1})	STY_{HCHO} ($g\,kg_{cat}^{-1}\,h^{-1}$)
Si 4-5P	50	3.5	78	16	6	1.0	0.78	310
F5	50	2.7	65	27	8	1.0	0.64	200
1-FS	50	8.6	55	28	17	0.50	0.28	534
2-FS	50	13.4	50	30	20	0.70	0.38	764
3-FS	50	13.2	39	30	31	0.07	0.03	586
FS-1	50	37.2	33	29	31	0.63	0.21	1395
FS-2	50	14.9	64	22	12	0.90	0.59	1060
FS-3	50	34.2	35	28	27	0.57	0.20	1351
FS-1	5	4.6	55	23	22	0.77	0.42	2872

[a] All the data have been obtained in batch reaction mode.
[b] Hourly conversion.

equal to 1.0 s^{-1}, though the lower S_{HCHO} of the latter system mirrors in a lower ε_{HCHO} (0.64 s^{-1}) with respect to the Si 45-P (0.78 s^{-1}). Evidently, a higher S_{CO} points out an enhanced tendency of such system to drive the consecutive oxidation of formaldehyde, probably because of the negative effect of the larger surface area (Table 1).

Addition of ca. 0.08 wt.% of Fe to the Si 4-5P silica sample by the INC/WET method (2-FS) implies a ca. four-fold rise in X_h (13.4%) along with a lowering in S_{HCHO} from 80 to 50% (Table 2), which account for a marked rise in STY_{HCHO} from 310 to 764 $g\,kg_{cat}^{-1}\,h^{-1}$. With reference to the Si 4-5P carrier, the above figures account for a decrease in σ_{CH_4} from 1.0 to 0.7 s^{-1} and, mostly, in the ε_{HCHO} value dropping to 0.38 s^{-1}. An equal amount of Fe (0.08 wt.%) added to F5 silica carrier still by INC/WET (1-FS) attains minor effects on activity (X_h, 8.6%), while the product distribution (S_{HCHO}, 55%) keeps similar to that of the above sample. Such a lower reactivity is indicated by a drop in σ_{CH_4} to 0.5 s^{-1} and ε_{HCHO} (0.28 s^{-1}) values, though the STY_{HCHO} (534 $g\,kg_{cat}^{-1}\,h^{-1}$) stays quite larger than that of carrier. By contrast, the FS-2 system, bearing 0.1 wt.% of Fe on F5 silica by ADS/PRC, displays a much higher activity (X_h, 14.9%) along with a high S_{HCHO} (64%), accounting for a σ_{CH_4} of 0.9 s^{-1} and a ε_{HCHO} of 0.59 s^{-1}. Although such figures well compare with those of silicas, as a consequence of a higher Fe content, the STY_{HCHO} abruptly rises to a value of 1040 $g\,kg_{cat}^{-1}\,h^{-1}$.

Addition of ca. 0.4 wt.% of Fe to the Si 4-5P carrier by INC/WET (3-FS) has a strongly negative effect on all the reactivity indices (S_{HCHO}, STY_{HCHO}, σ_{Fe}, ε_{HCHO}), as the 2-FS sample exhibits a σ_{CH_4} of only 0.066 s^{-1} coupled to a rather low S_{HCHO} (39%). As a consequence, a decrease in STY_{HCHO} (570 $g\,kg_{cat}^{-1}\,h^{-1}$) and a drop in ε_{HCHO} (0.026 s^{-1}) by more than one order of magnitude with respect to the 2-FS system are recorded (Table 2). This picture, implying quite high S_{CO} (30%) and S_{CO_2} (31%) values, is diagnostic of a very poor MPO functionality clearly due to a decay in FeO_x dispersion [4–9]. Indeed, though the comparable Fe loading (0.35 wt.%), the FS-1 sample (ADS/PRC) displays the highest activity (X_h, 37.2%), larger by ca. one order of magnitude than that of the relative silica carrier and ca. three-fold than that of the counterpart 3-FS catalyst. These data account for a σ_{CH_4} equal to 0.63 s^{-1}, while an S_{HCHO} (33%) comparable with that of the former system, results in a ε_{HCHO} value of 0.21 s^{-1} and the significant STY_{HCHO} of 1360 $g\,kg_{cat}^{-1}\,h^{-1}$. On the whole, the silica carrier plays a minor role on the reactivity of the active phase, as the FS-3 catalyst, bearing a similar amount of Fe (0.37 wt.% Fe) on F5 silica, exhibits a behaviour pattern analogous to that of the FS-1 system (Table 2). Though DR-UV-Vis data convey a higher dispersion of the active phase in the latter system, however, it must be emphasised that catalytic data on the whole well match with characterisation findings. In fact, the poor catalytic pattern of INC/WET samples is determined by the abundance of Fe_2O_3 *nanoparticles* accounting both for lower activity and unselective behaviour of INC/WET catalysts in MPO [4,7–9]. Whereas 2D $Fe^{(III)}O_x$ patches, mostly present on the FS-2 and FS-3 systems (Fig. 1), drive effectively the MPO reaction by providing ensembles of neighbouring active sites able to supply two oxygen atoms via a *four-electron-transfer* process [9,13,18].

Since the high activity of the FS-1 (and FS-3) catalyst resulting in reaction kinetics limited by the O_2 conversion level [9], the activity–selectivity pattern of the FS-1 catalyst was further probed at lower contact time (5 mg). In these conditions (Table 2), a hourly conversion comparable with that of the respective silica carrier and an S_{HCHO} of 55% are attained. These figures result in a σ_{Fe} equal to 0.77 s^{-1} and a ε_{HCHO} of 0.42 s^{-1}, while the STY_{HCHO} jumps to the value of 2872 $g\,kg_{cat}^{-1}\,h^{-1}$. Notably, such a figure results one order of magnitude greater than that of the carrier and more than five-fold larger than that of the counterpart 3-FS sample.

4. Conclusions

- DR-UV-Vis measurements of FeO_x/SiO_2 catalysts reveal the presence of "isolated" species, 2D "FeO_x patches" and 3D "Fe_2O_3 nanoparticles". Both preparation method and Fe loading control the *speciation* of active sites.
- The superior efficiency of the preparation route based on "adsorption–precipitation" of Fe^{II} precursors on silica

under anaerobic conditions (ADS/PRC) in enhancing the dispersion of FeO_x/SiO_2 catalysts is ascertained.
- The ADS/PRC method ensures a high dispersion of the active phase, conferring a considerably higher performance to FeO_x/SiO_2 catalysts in MPO in terms of Fe atoms specific activity, selectivity and HCHO productivity.

Acknowledgements

The financial support to this work by SUD CHEMIE AG (Munich, Germany) is gratefully acknowledged.

References

[1] R.W. Joyner, M. Stockenhuber, Catal. Lett. 45 (1997) 15.
[2] X. Feng, W.K. Hall, J. Catal. 166 (1997) 368.
[3] N. Mimura, M. Saito, Catal. Lett. 58 (1999) 59.
[4] T. Kobayashi, Catal. Today 71 (2001) 69.
[5] F. Arena, F. Frusteri, T. Torre, A. Venuto, A. Mezzapica, A. Parmaliana, Catal. Lett. 80 (2002) 69.
[6] F. Arena, F. Frusteri, L. Spadaro, A. Venuto, A. Parmaliana, Stud. Surf. Sci. Catal. 143 (2002) 1097.
[7] A. Parmaliana, F. Arena, F. Frusteri, A. Mezzapica, German Patent GEM 17 (2000) (Süd Chemie Ag).
[8] F. Arena, F. Frusteri, J.L.G. Fierro, A. Parmaliana, Stud. Surf. Sci. Catal. 136 (2001) 531.
[9] F. Arena, A. Parmaliana, Acc. Chem. Res. 36 (12) (2003) 867.
[10] S. Bordiga, R. Buzzoni, F. Geobaldo, C. Lamberti, E. Giamello, A. Zecchina, G. Leofanti, G. Petrini, G. Tozzola, G. Vlaic, J. Catal. 158 (1996) 486.
[11] G. Spoto, A. Zecchina, G. Berlier, S. Bordiga, M.G. Clerici, L. Basini, J. Mol. Catal. A 158 (2000) 107.
[12] B.K. Hodnett, Heterogeneous Catalytic Oxidation, Wiley, New York, 2000.
[13] V. Sokolovskii, Catal. Rev.-Sci. Eng. 32 (1990) 1.
[14] S. Albonetti, F. Cavani, F. Trifirò, Catal. Rev.-Sci. Eng. 38 (4) (1996) 413.
[15] K. Otsuka, Y. Wang, Appl. Catal. A 222 (2001) 145.
[16] J.L. Callahan, R.K. Grasselli, AIChE J. 9 (1963) 755.
[17] R.K. Grasselli, Top. Catal. 15 (2001) 93.
[18] K. Yoshizawa, Y. Shiota, T. Yamabe, J. Am. Chem. Soc. 120 (1998) 564.